Environment International 126 (2019) 279–288

Contents lists available at ScienceDirect

Environment International

journal homepage: www.elsevier.com/locate/envint

Mechanisms of algal biomass input enhanced microbial Hg methylation in lake sediments

Pei Lei[a,b,c], Luís M. Nunes[d], Yu-Rong Liu[e], Huan Zhong[c,f,*], Ke Pan[a,**]

[a] Institute for Advanced Study, Shenzhen University, Shenzhen 518060, China
[b] Key Laboratory of Optoelectronic Devices and Systems of Ministry of Education and Guangdong Province, College of Optoelectronic Engineering, Shenzhen University, Shenzhen 518060, China
[c] State Key Laboratory of Pollution Control and Resources Reuse, School of the Environment, Nanjing University, Nanjing 210046, China
[d] Civil Engineering Research and Innovation for Sustainability Center, University of Algarve, Faro, Portugal
[e] College of Resources and Environment, Huazhong Agricultural University, Wuhan 430070, China
[f] Environmental and Life Science Program (EnLS), Trent University, Peterborough, Ontario, Canada

ARTICLE INFO

Handling Editor: Frederic Coulon

Keywords:
Methylmercury
Organic matter
Eutrophication
Bioavailability
Algal blooms

ABSTRACT

Eutrophication is a major environmental concern in lake systems, impacting the ecological risks of contaminants and drinking water safety. It has long been believed that eutrophication and thus algal blooms would reduce methylmercury (MeHg) levels in water, as well as MeHg bioaccumulation and trophic transfer (e.g., by growth dilution). In this study, however, we demonstrated that algae settlement and decomposition after algal blooms increased MeHg levels in sediments (54–514% higher), as evidenced by the results from sediments in 10 major lakes in China. These could in turn raise concerns about enhanced trophic transfer of MeHg and deterioration of water quality after algal blooms, especially considering that 9 out of the 10 examined lakes also serve as drinking water sources. The enhanced microbial MeHg production in sediments could be explained by the algal organic matter (AOM)-enhanced abundances of microbial methylators as well as the input of algae-inhabited microbes into sediments, but not Hg speciation in sediments: (1) Several AOM components (e.g., aromatic proteins and soluble microbial by product-like material with generally low molecular weights), rather than the bulk AOM, played key roles in enhancing the abundances of microbial methylators. The copies of Archaea-*hgcA* methylation genes were 51–397% higher in algae-added sediments; thus, MeHg production was also higher. (2) Input of algal biomass-inhabited microbial methylators contributed to 2–21% of total Archaea-*hgcA* in the 10 lake sediments with added algal biomass. (3) However, AOM-induced changes in Hg speciation, with implications on Hg availability to microbial methylators, played a minor role in enhancing microbial Hg methylation in sediments as seen in X-ray absorption near edge structure (XANES) data. Our results suggest the need to better understand the biogeochemistry and risks of contaminants in eutrophic lakes, especially during the period of algae settlement and decomposition following algal blooms.

1. Introduction

Algal blooms are increasing in magnitude, frequency and duration globally (Huisman et al., 2018; Merel et al., 2013). The outbreak of algal blooms brings undesirable ecological consequences in lake ecosystems, such as deterioration of water quality and reduced biodiversity (Ger et al., 2016). Meanwhile, many studies have demonstrated that eutrophication could impact the biogeochemistry of pollutants (Camargo and Alonso, 2006; Tang et al., 2019), including methylmercury (MeHg) (He et al., 2008), a neurotoxin that biomagnifies along aquatic food chains (Carrasco et al., 2011; Tavshunsky et al., 2017). Algal blooms could mitigate MeHg bioaccumulation and trophic transfer, e.g., by growth biodilution (Noh et al., 2016; Pickhardt et al., 2002), removing MeHg from water column (Al-Reasi et al., 2007), or sequestrating MeHg in sediments by algal organic matter (AOM) (Soerensen et al., 2016).

However, a few pioneering studies have reported that AOM possibly facilitates microbial mercury (Hg) methylation in sediments (Bravo et al., 2017; Gascon et al., 2016; Herrero Ortega et al., 2018). For examples, the net Hg methylation rate is 10 times higher in settling algae

* Correspondence to: H. Zhong, School of Environment, Nanjing University, 163 Xian Lin Da Dao, Nanjing 210023, China.
** Correspondence to: K. Pan, Institute for Advanced Study, Shenzhen University, 3688 Nanhai Road, Shenzhen, Guangdong 518060, China.
E-mail addresses: zhonghuan@nju.edu.cn (H. Zhong), panke@szu.edu.cn (K. Pan).

https://doi.org/10.1016/j.envint.2019.02.043
Received 19 January 2019; Received in revised form 12 February 2019; Accepted 16 February 2019
Available online 27 February 2019

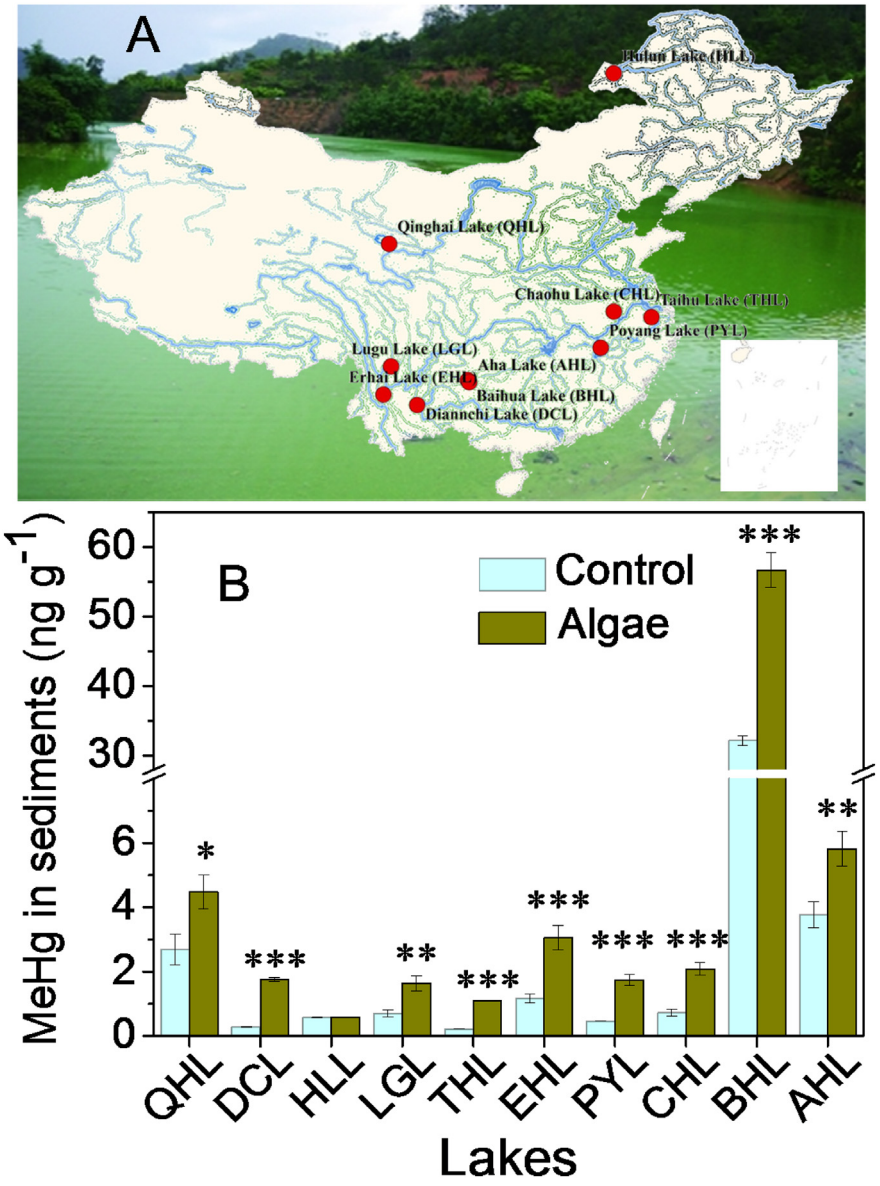

Fig. 1. Map showing the sampling sites of the 10 studied lakes in China (A). The changes of MeHg concentrations in lake sediments during a 21 day incubation (B). Error bars show standard errors, $n = 3$. The asterisk above the bars indicates a significant difference between 'Control' and 'Algae' treatment (one-way ANOVA, *, $p < 0.05$; **, $p < 0.01$; ***, $p < 0.001$; without *, $p > 0.05$). 'Algae': sediments from 10 studied lakes and unfiltered lake water amended with a certain level of algal biomass (i.e., 1000 mg L^{-1} in Experiment I) during a 21 day incubation; 'Control': the same lake sediments and unfiltered lake water with no algal biomass addition.

particles than surface sediments (Gascon et al., 2016). Bravo et al. also found that AOM increased Hg methylation rates in lake sediments (Bravo et al., 2017). These recent findings advance our understanding of Hg methylation in eutrophic lakes, and raise concerns about AOM-driven MeHg production and bioaccumulation. Unfortunately, the underlying mechanisms of enhanced Hg methylation are far from clear. The AOM-facilitated growth of microbial methylators in sediments has been suspected to be responsible for the enhanced microbial Hg methylation (Mazrui et al., 2016; Olsen et al., 2016). This could be possibly due to the different characteristics of AOM compared to sediment organic matter (e.g., humic and fulvic acids) (Bravo et al., 2017). To test this hypothesis, it is necessary to explore the connections between AOM characteristics (e.g., molecular weights and components) and microbial methylators in sediments (Mangal et al., 2019), especially during algae decomposition in sediments, when dynamic changes in AOM characteristics are noted (Han et al., 2015; Zhao et al., 2019). Recently, the identification of *hgcAB*, encoding Hg methylation genes in microbes (Gilmour et al., 2013; Parks et al., 2013), could greatly facilitate studies of AOM-impacted microbial methylators in sediments. This can help elucidate the possibly increased microbial MeHg production in eutrophic lakes.

In addition to AOM-facilitated growth of microbial methylators, algal biomass, which settles in large quantity and decomposes in sediments after algal blooms (Han et al., 2015), may enhance microbial Hg methylation by bringing algae-inhabited microbes into the sediments. High abundances of potential microbial methylators has recently been reported in biofilms or algae periphyton (Bouchet et al., 2018). This observation suggests the possibility that algae-inhabited microbes could increase the abundances of microbial methylators in sediments after algae settlement and thus enhance microbial MeHg production. Quantifying the changes in the abundances of *hgcA* methylation genes in sediments due to algae settling would help test this hypothesis.

The aim of this study was to test the hypothesis that settlement and decomposition of algal biomass into sediments could promote microbial

Hg methylation via two pathways: (1) increasing the abundances of microbial methylators in sediments by AOM input (as labile carbon sources for microbes) or (2) inputting algae-inhabited microbes into sediments. To test this idea, a series of microcosm experiments were conducted by using sediments from 10 major lakes in China, 9 of which also serve as drinking water sources. These lakes are subjected to widespread lake eutrophication (Huang et al., 2019; Wang, 2015), as well as high Hg emission and atmospheric deposition (Fu et al., 2012). Changes in the dynamics of AOM characteristics (molecular weights and components) were determined during algae decomposition in sediments. Potential microbial methylators in sediments or algal biomass were assessed by quantifying the abundances of *hgcA* gene. In addition, changes in Hg speciation in AOM-amended sediments were quantified with X-ray absorption near edge structure (XANES). The relationships among AOM characteristics, microbial methylators, and Hg speciation were then explored, to elucidate the mechanisms responsible for the enhanced Hg methylation in sediments after algal blooms.

2. Materials and methods

2.1. Field collection of algae and sediments

The algal biomass used here was collected at an algae gathering area of western part of Chaohu Lake. The Chaohu Lake, which suffers severe eutrophication, is the fifth largest freshwater lake in China (Jiang et al., 2014). The algal biomass was collected using a 112 μm mesh net and immediately transported back to laboratory with ice packs. The algal biomass was rinsed with distilled water for three times, freeze-dried, ground into fine power and stored at −20 °C before use. *Microcystis* spp. accounts for majority of algal biomass in Chaohu Lake during algal blooms (Jiang et al., 2014). Meanwhile, *Microcystis* spp. is also commonly reported as the dominant species during algal blooms in other freshwater lakes in China (Li et al., 2007; Luo et al., 2017; Tao et al., 2012; Yu et al., 2014), including those examined in this study (described below). Therefore, algal biomass collected from Chaohu Lake could be representative of those in most lakes investigated in this study.

The lake sediments were collected across a wide range of China (Fig. 1A). Ten lakes were selected, including Chaohu Lake (CHL), Qinghai Lake (QHL), Diannchi Lake (DCL), Hulun Lake (HLL), Lugu Lake (LGL), Taihu Lake (THL), Erhai Lake (EHL), Poyang Lake (PYL), Baihua Lake (BHL), and Aha Lake (AHL). Nine of the examined lakes serve as drinking water sources (except the salt water lake, QHL). The details of sampling sites are given in supporting information (SI) Table S1. For each lake, surface sediments (0–10 cm) were collected using a stainless steel grab sampler. The collected sediments were homogenized in situ, stored at 4 °C in the dark and immediately transported to the laboratory. The sediments samples were then air-dried for 3 days, ground and passed through a 0.15 mm (i.e., 100-mesh) sieve to remove large particles. The total mercury (THg) and MeHg concentrations in sediments or dried algal biomass were analyzed as described in Section 2.3 (Zhang et al., 2018) and the results are shown in SI Table S1.

2.2. Design of the microcosm experiments

A series of microcosm experiments were conducted to explore the effects of AOM addition on net MeHg production in lake sediments. The microcosm experiments contained three parts, each of which had a specific purpose: Experiment I and II were conducted to quantify the effects of AOM input on Hg methylation in sediments, while Experiment III was carried out to explore the underlying mechanisms responsible for AOM-impacted Hg methylation. Details of all treatments in Experiment I, II and III are summarized in SI Table S2.

Experiment I was carried out to quantify the net MeHg production in response to the AOM addition in 10 lake sediments from China, by comparing MeHg levels in sediments added or not with algal biomass. Specifically, 5 g (dry weight basis) of sediments were resuspended in 30 mL unfiltered lake water contained in a 50 mL polypropylene centrifuge tube (Corning, USA) within a glove bag (AtmosBag, Sigma Aldrich) filled with nitrogen gas (the same below in Experiment II and III). The algal biomass was added at a concentration of 1000 mg L^{-1}. This resulted in 40.0 ± 0.57 mg kg^{-1} chlorophyll *a* level in sediments, which was comparable to field observations from eutrophic lakes (Jiang et al., 2010). The THg and MeHg levels in the added algal biomass used in the experiments were 11.6 ± 0.10 ng g^{-1} and 1.693 ± 0.32 ng g^{-1}, respectively (SI Table S1). The tubes were capped tightly with parafilm and the mixtures were blended using a vortex mixer, after which the tubes were kept at 23 °C in an incubator without light (depicted in SI Fig. S1). Three replicates were made of each lake sediment ('Algae') and 'Control' to which no algal biomass was added. The incubation lasted for 21 days. At the end of the incubation, the tubes were opened within the glovebag filled with nitrogen gas, and pH and redox potentials (Eh) in water were determined using an HQ30d multi-parameter meters (HACH, USA). The mixtures were centrifuged at 4000*g* for 20 min and the supernatants were filtered with a 0.45 μm filter. The filtrates were determined for concentrations of dissolved organic carbon (DOC, Shimadzu TOC-VCPH analyzer) and sulfate (Dionex ICS1100, Thermo Fisher Scientific, USA). The MeHg concentrations in sediments were also analyzed.

Experiment II was conducted to quantify the net MeHg production in sediments in response to different levels of AOM input. This was achieved by comparing MeHg concentrations in the CHL sediments treated with different levels of algal biomass. Five grams of sediments from the CHL were resuspended in 30 mL unfiltered lake water, which was then mixed with 1500 ng of Hg (as $HgCl_2$). Hg was added into the CHL sediments in Experiment II (as well as Experiment III) to simulate the input of Hg into this lake systems, e.g., from atmospheric deposition or runoff (Fu et al., 2012; Jun et al., 2016; Ma et al., 2015), and to guarantee that the availability of inorganic Hg was not a limiting factor in Hg methylation. The added Hg levels (i.e., equivalent to 300 ng Hg g^{-1} sediment) were comparable with those levels in lake sediments in China (55.5 to 3019 ng g^{-1}, SI Tables S1). The Hg-spiked sediments were then added with different levels of algal biomass (0, 100 and 1000 mg L^{-1}) to mimic different eutrophic levels observed in the field. The amounts of algal biomass addition (quantified by the levels chlorophyll *a* in sediments were 17.8 ± 0.47, 21.5 ± 0.29, and 40.0 ± 0.57 mg kg^{-1}, respectively (SI Table S2). These were comparable to the values reported for eutrophic lakes (Jiang et al., 2010). Meanwhile, another set of samples treated as the ones above were spiked with methylation-inhibitor, i.e., Na_2MoO_4 (20 mM), to explore the potential role of SRB in Hg methylation in sediments (Bouchet et al., 2018; Gascon et al., 2016). Thus, a total of 6 treatments were studied in Experiment II. The mixtures were incubated for 21 days as those in Experiment I. At the end of the experiment, the sediment MeHg concentrations were measured and the sulfate concentrations in water were quantified.

Experiment III was carried out to explore the underlying mechanisms responsible for the AOM-facilitated microbial Hg methylation in sediments. This was achieved by quantifying (1) AOM characteristics (i.e., molecular weight distribution and fluorescence components), (2) abundances of potential microbial methylators in sediments (i.e., the copies of *hgcA* gene), and (3) Hg speciation in sediments. Briefly, 5 g of sediments from the CHL was resuspended in 30 mL lake water and mixed with algal biomass (1000 mg L^{-1}). Next, the mixtures were spiked with 1500 ng Hg like those in Experiment II. The incubation lasted for 56 days, during which DOC and sulfate levels in water were monitored on day 3, 7, 14, 28, 42, and 56. The molecular weight distribution and the fluorescence components of dissolved organic matter (DOM) in the supernatant were analyzed by high performance size exclusion chromatography (Waters, USA) and fluorescence excitation-emission matrix (Hitachi F-7000 Fluorescence Spectrophotometer), respectively (described below in Section 2.5). Besides, dissolved MeHg levels in the supernatant in Experiment III were determined. The MeHg

levels (described in Section 2.3), copies of *hgcA* gene (Archaea- and Deltaproteobacteria-*hgcA* gene, described in Section 2.4), HCl extractable Fe(II) (indicating iron reduction (Tong et al., 2014)) and concentrations of Chl*a* (indicating the eutrophication degree of lake sediments (Kowalewska, 2005), according to a spectrophotometric method described in previous reports (Hansson, 1988; Jiang et al., 2010)), were also analyzed in sediments at each sampling point.

The Hg speciation in sediments have implications on Hg bioavailability and thus microbial Hg methylation and were quantified by XANES. Specifically, sediments from Chaohu Lake (CHL, a typical shallow lake in Eastern China) and Baihua Lake (BHL, a typical deep-water lake in Western China) were selected from the 10 lakes, spiked with $HgCl_2$ (100 mg Hg kg^{-1} sediment), amended or not with algal biomass (1000 mg L^{-1} algal biomass), and incubated for 21 days like above. The relatively high spiked Hg levels in sediments (i.e., 100 mg THg kg^{-1}) were comparable to those in some contaminated lake sediments (Lin et al., 2010; Liu et al., 2012), and were commonly used to ensure detectable Hg levels by XANES (Wang et al., 2016). More details about XANES analysis were presented in SI Text S1.

2.3. Measurements of THg and MeHg in water and sediments

THg in sediments were determined by a Milestone DMA-80 Direct Mercury Analyzer according to USEPA Method 7473 (USEPA, 1998). The protocol for MeHg analysis of sediment and water samples has been reported elsewhere in details (Zhang et al., 2018; Zhu et al., 2016). Briefly, both the solid and aqueous samples were extracted with 25% KOH-methanol (w/w) and incubated at 60 °C for 4 h. The digests were then diluted with deionized water and analyzed for MeHg according to Method 1630 (USEPA, 2001) with an automatic MeHg analyzer (CVAFS, Brooks Rand model III, Brooks Rand Laboratories, USA). Quality control for MeHg measurements included method blanks, triplicates analyses, matrix spikes and the parallel analysis of certified reference materials (CRM), i.e., soil (ERM-CC580). The recoveries of MeHg were between 85 and 105% in the CRMs. Relative standard deviations of MeHg levels in water and sediments were 1.2–12.3% (averagely 7.4%) and 0.9–13% (averagely 8.5%), respectively.

2.4. DNA extraction and real-time quantitative PCR (qPCR) analysis

The total microbial DNA was extracted from 0.25 g sediment or algal samples using PowerSoil® DNA Isolation Kit (QIAGEN Inc., USA) based on the manufacturer's protocol, which was presented in details by (Liu et al., 2018). Briefly, the purity and concentration of isolated DNA were measured by a NanoDrop 2000 spectrophotometer (Thermo Fisher Scientific, USA), respectively, and then the DNA was stored at −20 °C before use.

The abundance of the *hgcA* gene was quantified using the clade-specific degenerate primer pairs ORNL-Archaea-HgcA for the Archaeal methylators and ORNL-Delta-HgcA for the Deltaproteobacterial methylators, respectively (Christensen et al., 2016), by amplification of the *hgc*A sequences from extracted DNA with an iCycler iQ5 thermocycler (Bio-Rad, USA). The primers for Archaea were ORNL-Archaea-HgcA-F (5′-AAYTAYWCNCTSAGYTTYGAYGC-3′) and ORNL-Archaea-HgcA-R (5′-TCDGTCCCRAABGTSCCYTT-3′). Primers of ORNL-Delta-HgcA-F (5′-GCCAACTACAAGMTGASCTWC-3′) and ORNL-Delta-HgcA-R (5′-CCSGCNGCRCACCAGACRTT-3′) were used for Deltaproteobacteria. The isolated DNA was diluted 10-fold and subjected to real-time quantitative PCR (also referred to qPCR) to obtain the abundance of *hgcA* genes in sediments. Each 25 μL reaction mixture contained 12.5 μL SYBR premix *Ex Taq* (TaKaRa Bio Inc., Japan), 0.5 μL each of 10 μM forward and reverse primers mentioned above and 2 μL of 10-fold diluted DNA template (1–10 ng). Optimized PCR thermal cycling parameters for Archaeal primers were set as following: 3 min initial denaturation at 95 °C, 40 cycles of 15 s at 95 °C, 30 s at 50 °C, and 25 s at 55 °C, 4 min at 72 °C, followed by a plate read at 83 °C. As for Deltaproteobacterial primers, the thermal-cycling conditions were set as: 3 min initial denaturation at 95 °C, 40 cycles of 15 s at 95 °C, 15 s at 50 °C, and 15 s at 55 °C, 4 min at 72 °C, followed by a plate read at 83 °C. Another five replicates, i.e., 25 μL reaction mixtures without template, were set as negative controls in the experiments.

Besides, PCR amplicons of *hgcA* genes from Archaea and Deltaproteobacteria were ligated to a pGEMT Easy vector (Promega, USA) and transformed into *Escherichia coli* JM109 cells (TaKaRa Bio Inc., Japan) according to the manufacturer's protocols, in order to check amplicon sequences and obtain a standard curve for quantification. Then, positive clones containing the target gene insert were sequenced, and the most abundant one was used for plasmid DNA extraction. After measuring the DNA concentration by using a Nanodrop ND-1000 UV–visible spectrophotometer (NanoDrop Co., USA), the purified plasmid DNA was diluted serially in 10-fold steps and subjected to qPCR in triplicate to generate an external standard curve (Ma et al., 2017).

2.5. Analysis of molecular weight distribution and fluorescence components of DOM

Molecular weight distributions were determined by high performance size exclusion chromatography (HPSEC) (Chow et al., 2008; Xing et al., 2012). The mobile phase was Milli-Q water buffered with 5 mM phosphate to pH 6.8, and 0.01 M NaCl was filtered through a 0.22 μm membrane, and then degassed for 30 min. The flow rate was 0.8 mL min^{-1} and the injection volume was 200 μL. The system was calibrated with PSS standards and DOM samples were detected at at 254 nm.

Optical properties of DOM were measured on a Hitachi F-7000 Fluorescence Spectrophotometer. The five resulting components across the EEMs were expressed as the Region I for Aromatic Protein I (API, λ_{ex}: 220–250 nm, λ_{em}: 280–330 nm), Region II for Aromatic Protein II (APII, λ_{ex}: 220–250 nm, λ_{em}: 330–380 nm), Region III for Fulvic acid-like (FA, λ_{ex}: 220–250 nm, λ_{em}: 380–550 nm), Region IV for Soluble microbial by-product-like (SMP, λ_{ex}: 250–340 nm, λ_{em}: 280–380 nm) and Region V for Humic acid-like (HA, λ_{ex}: 250–280 nm, λ_{em}: 280–550 nm) (Chen et al., 2003). Fluorescence region integration (FRI) was conducted to quantify semi-quantitative components of DOM and explore the relationships between the copies of Archaea-*hgcA* gene in sediments and DOM components.

2.6. Statistical analysis

The one-way analysis of variance (ANOVA) with Tukey's multiple comparison test were applied to compare the statistical significance among multiple treatments. The asterisk above the bars indicates significant difference among treatments, i.e. *, $p < 0.05$; **, $p < 0.01$; ***, $p < 0.001$; without *, $p > 0.05$. Besides, a Principal Component Analysis (PCA) was made to explore the multivariate relationships among the physical-chemical parameters of sediments, Hg methylation, and the presence of Hg methylators in the 10 studied lakes. The best outcome of PCA came when the following variables were included: pH, Eh, HCl extractable Fe(II), sulfate, DOC, THg, MeHg, and Archaea-*hgcA* gene copies.

3. Results and discussion

3.1. Enhanced MeHg levels in sediments following algae addition

There were increased MeHg levels in sediments following algae addition ('Algae' versus 'Control'): (1) Algae addition resulted in 54–514% increases (average of 207%) in MeHg levels in sediments collected from the 10 major lakes in China (Fig. 1B). Despite the variations in sediment characteristics and ambient Hg concentrations (SI Table S1), the only exception was the sediments from HLL, in which MeHg levels were comparable despite the algae addition ($p > 0.05$).

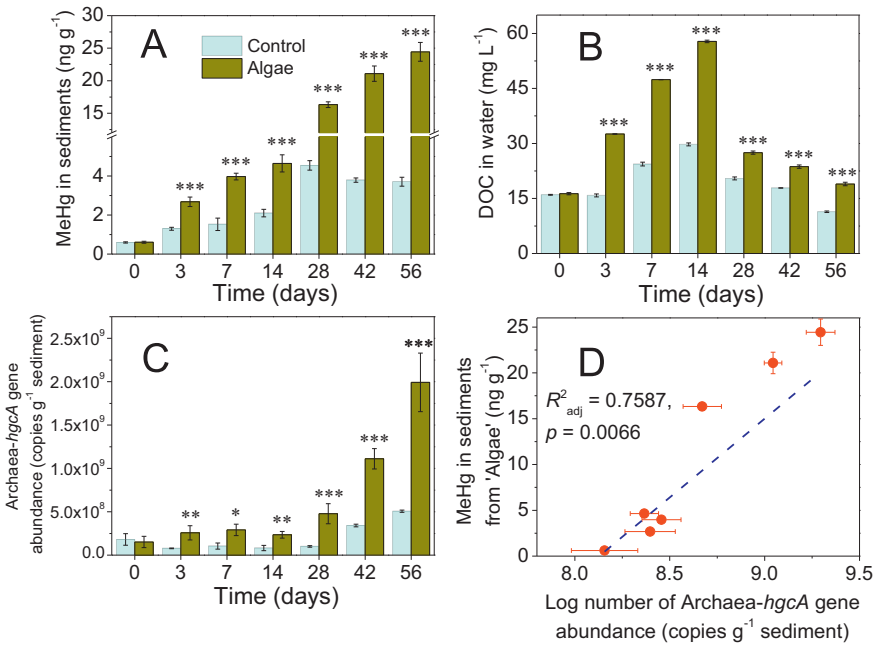

Fig. 2. Changes of MeHg concentrations (A) in Chaohu lake (CHL) sediments and DOC contents in water (B) as well as the copies of Archaea-*hgcA* gene (C) in sediments and linear relationship of MeHg levels and Archaea-*hgcA* gene copies in 'Algae' treatments (D) during the 56 day incubation. Error bars show standard errors, $n = 3$. The asterisk above the bars indicates significant difference between 'Control' and 'Algae' treatment (one-way ANOVA, *, $p < 0.05$; **, $p < 0.01$; ***, $p < 0.001$; without *, $p > 0.05$). 'Algae': sediments from CHL and unfiltered lake water amended with a certain level of algal biomass (i.e., 1000 mg L^{-1} in Experiment III) during a 56 day incubation; 'Control': the lake sediments and unfiltered lake water with no algal biomass addition.

The higher MeHg levels in sediment from BHL (24.8 ± 1.77 ng g^{-1} versus 0.152 ± 0.021–1.62 ± 0.178 ng g^{-1} in other sediments) were mainly because of the higher ambient THg levels in BHL (3019 ± 186 ng g^{-1} versus 55.5 ± 1.24–238 ± 15.1 ng g^{-1} in other sediments, SI Table S1), which was historically contaminated by high-Hg industrial wastewater (Yan et al., 2013). (2) MeHg levels were 47% and 306% higher ($p < 0.05$) in the Chaohu lake (CHL) sediments added with lower (100 mg L^{-1}) or higher (1000 mg L^{-1}) amount of algal biomass (SI Fig. S5A). This may represent algae settling into sediments after different degrees of eutrophication. (3) MeHg concentrations were 106–559% higher in the CHL sediments added with algae from 0 to 56 day incubation period (Fig. 2A). Besides, dissolved MeHg levels in the overlying water were 269–1077% higher after algae addition (SI Fig. S4A).

The responses of MeHg production to algae addition varied among the examined sediments: as low as 1% in the HLL and as high as 400% in the THL. The different responses could be partially attributed to the ambient organic matter contents in different sediments: the increases of MeHg levels due to algae addition (i.e., MeHg levels in 'Algae' - MeHg levels in 'Control') decreased linearly with the levels of loss on ignition (LOI) in sediments (indicating ambient organic matter contents (Santisteban et al., 2004)), after excluding data points of the HLL (SI Fig. S2A). These results demonstrate that the algae addition-facilitated microbial MeHg production was more obvious in sediments with lower organic matter content. The only exception was the HLL sediment, in which LOI was the lowest (3.7%); algae addition had only minor effects on the MeHg levels in the sediments. The inconsistency between the HLL and other sediments is largely unexplained and should be further explored in future studies. Meanwhile, the increased MeHg levels in the 10 studied sediments following algae addition should not be mainly attributed to input of algae-associated Hg, considering that: (1) The amount of MeHg in added algal biomass (ng) contributed to < 1.7% of MeHg in algae-added sediments (ng); (2) The amount of THg in added algal biomass (ng) was < 0.13% of ambient THg in different lake sediments (ng).

Our results suggest that algae settlement and decomposition could increase MeHg production in sediments, and the mechanisms were further elucidated in Section 3.2–3.4. These findings, together with recent evidences of AOM-enhanced MeHg production (Bravo et al., 2017; Herrero Ortega et al., 2018), question the common belief that algal blooms reduce the risk of MeHg in aquatic systems (e.g., by bio-dilution (Pickhardt et al., 2002)), considering that MeHg levels in different sediments increased after the blooms. These observations also dispute the assumption that AOM input into sediments may reduce microbial Hg methylation by binding strongly with Hg in sediments (Driscoll et al., 2012).

Indeed, we show that MeHg production increased following algae settlement and decomposition in sediments. China has approximately 8700 km^2 of eutrophic lakes, and the area approaching eutrophication is about 14,000 km^2 (Wang, 2015). Meanwhile, China has among the highest Hg emission and atmospheric deposition rates (Fu et al., 2012). Therefore, eutrophication-driven increases in MeHg production in sediments may subsequently enhance dissolved MeHg levels (SI Fig. S4A) and thus trophic transfer of MeHg in water column (Chiasson-Gould et al., 2014; French et al., 2014), which could be underestimated previously and warrant further investigation, especially field survey. Besides, the enhanced MeHg levels in sediments and thus the partitioning of MeHg into water column (Fig. 2A & SI Fig. S4A), could impact water quality, raising health concerns (Hsu-Kim et al., 2013; Klapstein and O'Driscoll, 2018).

3.2. Increased abundances/activities of microbial methylators explain enhanced MeHg production

The elevated MeHg levels in sediments after algae addition could be mainly attributed to the increased abundances (quantified by *hgcA* copies) or activities (indicated by either sulfate reduction or iron reduction) of potential microbial methylators, but not Hg speciation in sediments:

(1) The copies of Archaea-*hgcA* gene in the sediments, indicating the abundances of potential microbial methylators (e.g., methanogens (Liu et al., 2018)), were 51–397% higher in 8 out of 10 sediments added with algae ('Algae' versus 'Control', $p < 0.05$, SI Fig. S3C). Meanwhile, the increment of MeHg levels (i.e., MeHg levels in 'Algae' sediments minus MeHg levels in 'Control' sediments) increased linearly with the increment of Archaea-*hgcA* copies, (i.e., Archaea-*hgcA* copies in 'Algae' sediments minus the copies in 'Control' sediments, SI Fig. S2B). Similarly, the copies of Archaea-*hgcA* were significantly higher ($p < 0.05$) in the CHL sediments added with algae during the 56 day incubation period (Fig. 2C). MeHg levels in sediments from 'Algae' treatments increased with

the copies of Archaea-*hgcA* (R_{adj}^2 = 0.7587, p = 0.0066, Fig. 2D).

Similar to Archaea-*hgcA*, the copies of Deltaproteobacteria-*hgcA* (e.g., sulfate/iron reducing bacteria, (Liu et al., 2018)) (SI Fig. S3D & SI Fig. S4B), which were approximately 1 order lower than Archaea-*hgcA* (Fig. 2C & SI Fig. S3C), generally increased following algae addition. However, MeHg levels were not significantly correlated with the copies of Deltaproteobacteria-*hgcA* ($p > 0.05$, SI Fig. S2C & SI Fig. S4E). Therefore, we mainly focused on exploring potential controls of Archaea-*hgcA* on MeHg levels in sediments. More discussions about Deltaproteobacteria-*hgcA* could be found in SI Text S3.

The above observations all support that AOM-promoted MeHg production could be mainly attributed to the increased abundances of potential microbial methylators (e.g., methanogens, sulfate reducing bacteria, and iron reducing bacteria) in sediments.

(2) In addition to increased copies of *hgcA* gene, activities of potential microbial methylators also increased following algae addition. In all examined sediments, dissolved sulfate levels were 38–67% lower in 'Algae' sediments ($p < 0.05$, SI Fig. S3B) than 'Control', suggesting enhanced activities of SRB and thus sulfate reduction (Correia and Guimarães, 2016). Similarly, dissolved sulfate levels were lower ($p < 0.05$) in the CHL sediments added with algae during the 56 day incubation period (SI Fig. S4C). Meanwhile, HCl extractable Fe(II) levels, indicating the activities of iron-reducing bacteria (FeRB) (Lee et al., 2012) were significantly higher after algae addition in 5 out of 10 sediments ($p < 0.05$, 'Algae' versus 'Control', SI Fig. S3G) after 21 days of incubation.

In addition to microbial methylators, speciation and thus bioavailability of Hg (to microbial methylators) in sediments could also affect microbial Hg methylation (Zhong and Wang, 2010). However, Hg speciation in sediments analyzed by XANES may not be mainly responsible for the increased Hg methylation following algae addition, considering the minor changes in Hg speciation, e.g., HgS and Hg-OM (SI Fig. S6 & SI Table S3). Particularly, AOM input could not increase Hg-OM in sediments. This could be attributed to relatively low contribution of AOM input to the organic matter content in sediments, considering that LOI is 3.6–9.7% (SI Fig. S2A) in sediments while added algae/sediment was 0.6% (w/w) in most treatments. More discussions could be found in SI Text S2.

To further explore the potential relationships between microbial methylators (indicated by the Archaea-*hgcA* copies, SI Fig. S3C) and parameters related to microbial methylators or Hg methylation (THg and MeHg in SI Table S1; HCl extractable Fe(II), sulfate and DOC in SI Fig. S3G, 3B & 3A; pH & Eh in SI Fig. S3E & 3F), a PCA analysis was made for the 10 studied lake sediments. Together they reflect the broad physical-chemical condition of the media, the availability of electron donors (DOC) and acceptors (Fe and sulfate), the presence of the main Hg species, and Hg methylators.

The results of PCA indicated that three eigenvalues were larger than 1.0 with a cumulative explained variance of 80.4% (SI Table S4). Therefore, only these first three factors were used in the subsequent analysis. Variable-factor correlations indicate that Factor 1 is essentially a linear combination of pH, Eh, THg and MeHg, and to a lesser extent also of DOC; while Factor 2 is of the variables of Archaea-*hgcA* copies, sulfate, and to a lesser extent also of DOC (SI Table S5). Thus, the former can help classify the samples as to the presence of Hg species under broad physical-chemical conditions. For instance, more reducing environments and higher THg levels promote methylation (negative and positive correlations with the factor, respectively) (Klapstein and O'Driscoll, 2018). The latter helps to classify samples according to microbial methylation, with sulfate reduction playing the main role in controlling the presence of Hg methylators (i.e., the *hgcA* genes) (Zeng et al., 2016). This may further evidence the key role of SRB in controlling microbial Hg methylation.

Interestingly, DOC has a pivotal role between the two broad processes explained by the two factors: the relatively low and similar correlation between them and DOC indicates that DOC may play a critical role in microbial Hg methylation (Chiasson-Gould et al., 2014). The introduction of algal biomass could promote a shift in its physical-chemical conditions of the medium in the methylation, which is very well captured by the studied variables. This is indicated by the quite different scores in the factorial space (SI Fig. S7). In view of those results, the mechanisms of algae addition-facilitated Hg methylation in sediments were further explored in Section 3.3, focusing on the controls of DOC on microbial methylators and thus microbial Hg methylation.

3.3. AOM input increased the abundances of microbial methylators in sediments

The above results highlight the importance to elucidate increases in the abundances of microbial methylators in sediments following algae settling and decomposition. Here, we propose that (1) certain components of AOM, rather than the bulk AOM could be responsible for the increased abundances of microbial methylators in sediments after algae addition (discussed in this section). We further suggest that (2) microbes inhabited in settled algal biomass could also contribute to increase the abundances of microbial methylators in sediments (discussed in Section 3.4).

The increased abundances of microbial methylators could be explained by the increased supply of labile carbon via AOM input (as electron donor (Mazrui et al., 2016)). Concentrations of DOC increased by 18–104% in the 10 examined lake sediments after 21 day incubation with algae (SI Fig. S3A) and 33–106% in the CHL sediment during the 56 day incubation (Fig. 2B). Besides, more discussion about the dynamics of DOC levels following algae addition could be found in SI Text S4. However, the increased DOC levels alone may not explain the enhanced abundances of microbial methylators and thus MeHg production, in view of the contradictory effects of DOM on microbial MeHg production: On one hand, DOM could facilitate microbial Hg methylation by enhancing the activities of heterotrophic microorganisms (Parks et al., 2013). Besides, complexes between some low molecular weight (LMW) DOM and Hg could be taken up by microbial methylators and facilitate Hg methylation (Leclerc et al., 2015; Zhao et al., 2018). On the other hand, some DOM with high molecular weight could complex with Hg, and the complexes were found to be unavailable to microbial methylators (Chiasson-Gould et al., 2014). This 'double-edged sword effect' of DOM on microbial Hg methylation has been widely reported in aquatic systems (French et al., 2014; Klapstein and O'Driscoll, 2018; Luengen et al., 2012), and could be commonly attributed to the differences in molecular weights and components of DOM.

Therefore, we analyzed both the molecular weight distribution (SI Fig. S8) and components (indicated by specific fluorescence characteristics, SI Fig. S9) of AOM to elucidate the effects of AOM on the abundances of microbial methylators and thus MeHg production. Briefly, the concentrations of DOC in < 1 kDa fraction were 16–150% higher (average of 81%) in 'Algae' (SI Fig. S10). Consequently, the increases in LMW DOM (< 1 kDa) following algae addition could possibly facilitate Hg methylation, considering the following: (1) LMW DOM has been commonly reported to enhance microbial activities by providing labile carbon (Mazrui et al., 2016). (2) Complexes between some LMW DOM (e.g., thiols) and Hg are directly taken up by microbial methylators to enhance MeHg production (Chiasson-Gould et al., 2014; Leclerc et al., 2015). For instance, a recent laboratory study found that increases in Hg uptake by *Escherichia coli* were positively correlated to LMW DOM (i.e., amino acids and polyamines) harvested from algal DOM (Mangal et al., 2019).

In addition to the molecular weights, DOM component is another key factor controlling the abundances of microbial methylators and thus microbial MeHg production (Bravo et al., 2017; Herrero Ortega

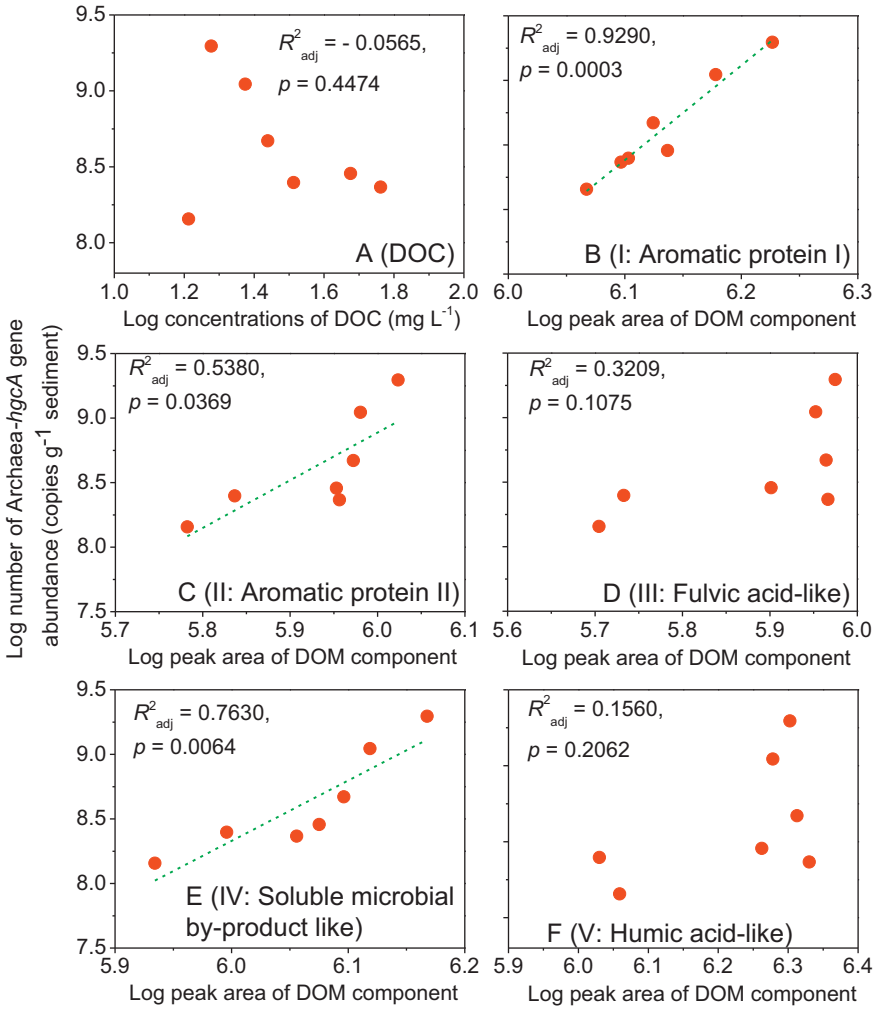

Fig. 3. Linear relationships between the copies of Archaea-*hgcA* gene in sediments and DOC concentrations (A) and the amount of five components of DOM (A-F) in 'Algae' treatments. 'Algae': sediments from Chaohu lake (CHL) and unfiltered lake water amended with a certain level of algal biomass (i.e., 1000 mg L^{-1} in Experiment III) during a 56 day incubation.

et al., 2018). The peak areas of the five components (indicating the amount of different AOM components (Chen et al., 2003)) in 'Algae' treatments were all higher than those in 'Control' (SI Fig. S11). These are mainly attributed to the decomposition and transformation of AOM in sediments.

There was no significant relationship between DOC levels and the Archaea-*hgcA* gene copies for either 'Algae' or 'Control' ($p > 0.05$, Fig. 3A & SI Fig. S12A). However, for 'Algae' treatments, significant relationships were found between the Archaea-*hgcA* copies and the amounts of Aromatic Protein I, II (API, APII: aromatic proteins such as tyrosine and tryptophan (Chen et al., 2003, Zhang et al., 2015)), or soluble microbial by product-like material (SMP): $R^2_{adj} = 0.9290$, 0.5380, or 0.7630 ($p < 0.05$, Fig. 3B, C & 3E). Meanwhile, there was no correlation between the copies of Archaea-*hgcA* and the amounts of humic substances (HA) or fulvic acid-like substances (FA) for 'Algae' treatments ($p > 0.05$, Fig. 3D & 3F).

The inconsistent relationships between different AOM components (API, APII and SMP vs. HA and FA) and the copies of Archaea-*hgcA* gene could be explained by their different molecular weights and thus availability to microbial Hg methylators: Recent studies reported that the protein fluorescence was highest at lower molecular weights (< 0.5 kDa), while the fulvic or humic-like fluorescence was highest at larger molecular weights (> 1 kDa) (Cuss and Guéguen, 2015). Therefore, the AOM as API, APII (aromatic proteins such as tyrosine (Chen et al., 2003)) and SMP (e.g., tryptophan phenylalanine or tryptophan (Dignac et al., 2000)), with generally low molecular weights, might serve as labile carbon sources for microbial methylators. Similarly, a recent study also showed that the bioavailable DOM (80% of DOC) derived from algae decomposition were protein-like components. They were less aromatic, nitrogen-rich, and more oxygenated smaller molecules and preferentially utilized by microorganisms. In contrast, the humic-like fluorescent components, primarily composed of carboxylic-rich alicyclic compounds, exhibited bioresistant behavior (Bai et al., 2017). These results, together with the molecular weights of the AOM discussed above, could help elucidate the enhanced *hgcA* abundances and thus Hg methylation in sediments following algae settling and decomposition.

Our results highlight the key role of several AOM components (i.e., API, APII, and SMP) in microbial methylators and thus MeHg production in sediments during algae decomposition, while the total concentrations of DOM (i.e. indicated by DOC concentrations) may play a minor role. Similarly, high Hg methylation rates have been attributed to algal and/or microbial DOM (e.g., labile and protein-like DOM) with lower molecular weight in aquatic systems (Bravo et al., 2017; Gascon et al., 2016; Herrero Ortega et al., 2018; Lescord et al., 2018; Mazrui et al., 2016). Our findings might also help explain the inconsistent relationships between MeHg production and DOC levels commonly reported in aquatic systems (French et al., 2014). For example, positive (Bravo et al., 2018; Hill et al., 2009), negative (Jeremiason et al., 2016; Luengen et al., 2012) and insignificant relationships (Lescord et al.,

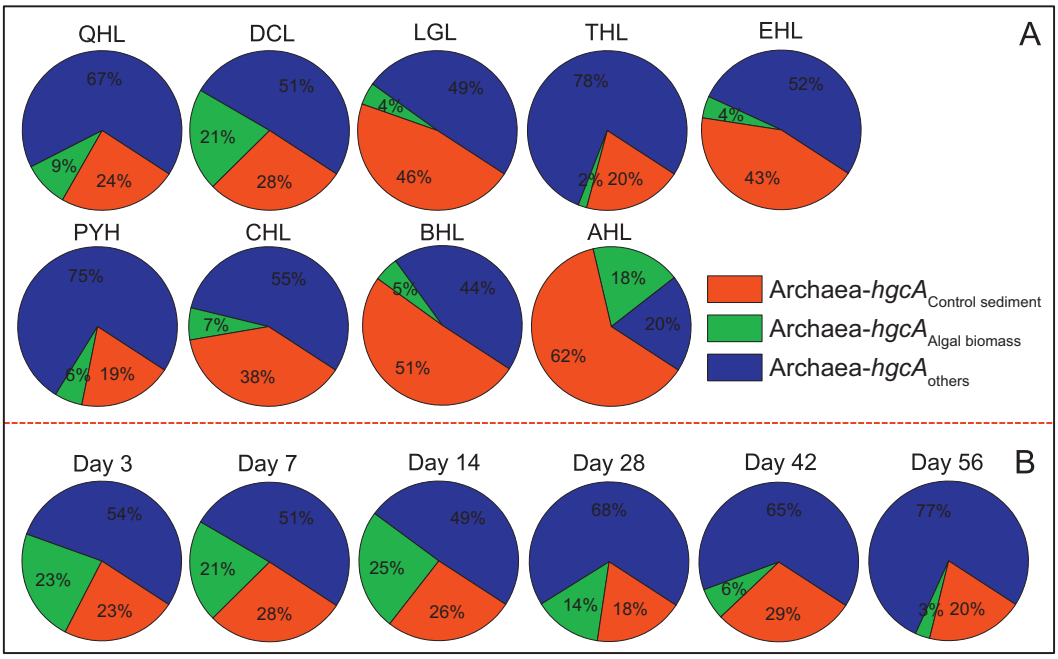

Fig. 4. Contributions of Archaea-*hgcA* copies in 'Algae' sediments of 9 major lakes (A) and the Chaohu Lake after 56 day incubation (B). $hgcA_{\text{algal biomass}}$, $hgcA_{\text{Control sediment}}$, and $hgcA_{\text{Other}}$ are for copies of Archaea-*hgcA* in algal biomass (equivalent to the copies g^{-1} sediment), 'Control' sediment and other unknown origins, respectively. The data from the HLL sediments and day 0 in the CHL sediments were excluded because the sum of $hgcA_{\text{algal biomass}} + hgcA_{\text{Control sediment}}$ was large than the $hgcA_{\text{algae-added sediment}}$. 'Algae': sediments from 10 studied lakes and unfiltered lake water amended with a certain level of algal biomass (i.e., 1000 mg L^{-1} in Experiment I and III); 'Control': the same lake sediments and unfiltered lake water with no algal biomass addition.

2018) were found between MeHg production and DOC levels in aquatic systems. Further studies in linking DOM characteristics (e.g., molecular weights and components) and microbial methylators are necessary, to better interpret or predict microbial MeHg production in eutrophic lakes. While AOM input could facilitate Hg methylation during algae decomposition, microbial Hg methylation in sediments and in water column during algal blooms is less understood and should be further investigated in future studies. Particularly, AOM may play the dual roles in microbial Hg methylation, i.e., (1) by binding strongly with Hg and inhibit Hg methylation, and (2) by providing labile carbon to microbes and thus facilitate microbial Hg methylation. Therefore, differences in AOM compositions/molecular weights during and after algal bloom may impact the net effects of AOM input on Hg methylation, which warrant further investigation.

3.4. Input of algae-inhabited microbes into sediments increased the abundances of microbial methylators in sediments

In addition to AOM-enhanced microbial abundances and thus MeHg production in sediments, algae-inhabited microbes and their input into sediments following algae settlement could also be responsible for the increased abundances of microbial methylators and thus MeHg production. Algae has a large surface area (Tao et al., 2012), with high capacity for Hg adsorption (Al-Reasi et al., 2007). Besides, high levels of labile carbon (e.g., extracellular polymeric substances, EPS) are commonly found on the cell surface of algae (Leclerc et al., 2015), where microorganisms (including potential microbial methylators of Hg, e.g., SRB) could inhabit (Bouchet et al., 2018). Therefore, algae particles could potentially be a 'hotspot' of microbial MeHg production (Tsui et al., 2010), either by direct methylation of Hg or by releasing metabolites (i.e., labile carbon, LMW thiols, or both) and thus enhancing bacterial activities and/or inorganic Hg bioavailability (Bouchet et al., 2018; Olsen et al., 2016). For example, a previous study reported elevated MeHg levels in settling algae particles in Lake Geneva versus surface sediments, although the THg concentrations were comparable (Gascon et al., 2016). In addition, the Hg methylation potential (calculated by the ratio of Hg methylation rate and demethylation rate) was 10-fold higher in settling algae particles than surface sediments (Gascon et al., 2016).

Here, the settled algae particles could facilitate microbial MeHg production in sediments via input of algae-inhabited microbial methylators due to several features.

(1) The copies of Archaea-*hgcA* methylation gene reached 1.27×10^{10} copies g^{-1} dry algal biomass, approximately 10–100 times higher than those in sediments of 'Control' (e.g., 1.99×10^{8}–2.12×10^{9} copies g^{-1} sediment in Experiment I for different sediments (SI Fig. S3C) and 7.82×10^{7}–5.06×10^{8} copies g^{-1} sediment in Experiment III for CHL sediment) (Fig. 2C). Consequently, the increases in Archaea-*hgcA* copies in sediments due to algae addition (i.e., equivalent to $7.64 \times 10^{7} \pm 1.77 \times 10^{7}$ copies g^{-1} sediment) were comparable to Archaea-*hgcA* copies in sediments of 'Control'. These inputted microbial methylators could subsequently enhance microbial MeHg production in sediments as observed in this study. Similarly, a very recent study suggests that the presence of *hgcAB* genes in algae periphyton might explain the higher Hg methylation in planktonic particles versus sediments (Bouchet et al., 2018).

(2) While positive relationships were found between Archaea-*hgcA* copies in sediments and the amount of API, APII and SMP in 'Algae' treatments, no such relationship was found in 'Control' (SI Fig. S12). This suggests that DOM components alone might not fully explain the variations in Archaea-*hgcA* copies in sediments, or the differences in Archaea-*hgcA* copies between 'Algae' and 'Control'. Rather, algae-inhabited microbial methylators and their input into sediments could also contribute to Archaea-*hgcA* in algae-added sediments.

(3) To further explore the relative importance of algae-inhabited microbial methylators and their input into sediments, we calculated the relative contribution (C_{hgcA}, %) of algal biomass-inhabited or sediment inherent microbial methylators to total Archaea-*hgcA* in sediments added with algae:

$$C_{hgcA} = \frac{hgcA_{algal\ biomass}\ (or\ hgcA_{Control\ sediment})}{hgcA_{algae\text{-}added\ sediment}} \times 100$$

Here, $hgcA_{\text{algal biomass}}$ stands for copies of Archaea-*hgcA* in algal biomass (equivalent to the copies g^{-1} sediment), $hgcA_{\text{algae-added sediment}}$ is the copies of Archaea-*hgcA* in algae-added sediment, and $hgcA_{\text{Control sediment}}$ is the copies of Archaea-*hgcA* in 'Control' sediment.

We found that the algal biomass-inhabited microbial methylators ($hgcA_{\text{algal biomass}}$) contributed to 2–21% of total Archaea-*hgcA* in the 10 sediments added with algae (Fig. 4A), and 3–25% in algae-added CHL sediment incubated for different times (Fig. 4B). This provides further evidence that the microbial methylators inputted with settled algal biomass might also enhance Archaea-*hgcA* in sediments, thus facilitating microbial Hg methylation. Meanwhile, the $hgcA_{\text{algae-added sediment}}$ values were 2–351% and 67–242% higher than $hgcA_{\text{algal biomass}} + hgcA_{\text{Control sediment}}$ in most sediments (except HLL) and in the CHL sediment (except day 0), respectively. This shows that algae-associated Archaea-*hgc*A is not the only reason for the increased Archaea-*hgc*A in sediments. In fact, the AOM-facilitated growth of microbial methylators could be evidenced by the high percentages of '$hgcA_{\text{other}}$' (20–78% in Fig. 4A and 49–77% in Fig. 4B). It would be interesting to further compare the increases in inherent microbial methylators in sediments and algal biomass-inhabited microbial methylators, in response to AOM input.

4. Conclusions

This study explored the effects of algae decomposition on Hg methylation in eutrophic lake sediments. We provide evidence that both AOM-enhanced microbial methylators and the input of algae-associated microbial methylators could contribute to the increases in *hgcA* genes in sediments and thus microbial MeHg production. Particularly, we demonstrate that several AOM components (i.e., API, APII and SMP), rather than the bulk AOM, played key roles in enhancing the abundances of microbial methylators. Our results also suggest that ignorance or underestimation of algae-inhabited microbial methylators could possibly lead to failures in predicting the risk of MeHg production in sediments. These observations together with mechanistic explanations suggest the need of better understanding the biogeochemistry and the risks of contaminants in eutrophic lake systems, especially during algae decomposition following algal blooms.

Declaration of interests

The authors have no competing or conflicting interests in relation to the issues tackled in this paper.

Acknowledgements

This study was supported by the China Postdoctoral Science Foundation [grant number 2017M622782], the National Natural Science Foundation of China [grant numbers 41676095, 41673075] and the Natural Science Foundation of Jiangsu Province [grant number BK20160067]. In-kind support of field sample collection was provided by X.H. Kong and Dr. W.Q. Zhang. Laboratory and data analysis support were provided by X.Q. Zhou, Dr. Y.J. Wang, Dr. H. Li and Dr. H. Xu. Hg L_{III}-edge XANES determination was supported by Shanghai Synchrotron Radiation Facility (SSRF, China). We also thank the anonymous reviewers for their constructive comments and suggestions.

Appendix A. Supplementary data

Supplementary data to this article can be found online at https://doi.org/10.1016/j.envint.2019.02.043.

References

Al-Reasi, H.A., Ababneh, F.A., Lean, D.R., 2007. Evaluating mercury biomagnification in fish from a tropical marine environment using stable isotopes (δ13C AND δ15N). Environ. Toxicol. Chem. 26 (8), 1572–1581.
Bai, L.L., Cao, C.C., Wang, C.H., Xu, H.C., Zhang, H., Slaveykova, V.I., Jiang, H.L., 2017. Toward quantitative understanding of the bioavailability of dissolved organic matter in freshwater lake during *Cyanobacteria* blooming. Environ. Sci. Technol. 51 (11), 6018–6026.
Bouchet, S., Goñi-Urriza, M., Monperrus, M., Guyoneaud, R., Fernandez, P., Heredia, C., Tessier, E., Gassie, C., Point, D., Guédron, S., 2018. Linking microbial activities and low molecular weight thiols to Hg methylation in biofilms and periphyton from high altitude tropical lakes (Bolivian altiplano). Environ. Sci. Technol. 52 (17), 9758–9767.
Bravo, A.G., Bouchet, S., Tolu, J., Björn, E., Mateosrivera, A., Bertilsson, S., 2017. Molecular composition of organic matter controls methylmercury formation in boreal lakes. Nat. Commun. 8, 14255.
Bravo, A.G., Kothawala, D.N., Attermeyer, K., Tessier, E., Bodmer, P., Ledesma, J.U., Audet, J., Casas-Ruiz, J.P., Catalan, N., Cauvy-Fraunie, S., Colls, M., Deininger, A., Evtimova, V.V., Fonvielle, J.A., Fuss, T., Gilbert, P., Ortega, S.H., Liu, L., Mendoza-Lera, C., Monteiro, J., Mor, J.R., Nagler, M., Niedrist, G.H., Nydahl, A.C., Pastor, A., Pegg, J., Roberts, C.G., Pilotto, F., Portela, A.P., Gonzalez-Quijano, C.R., Romero, F., Rulik, M., Amouroux, D., 2018. The interplay between total mercury, methylmercury and dissolved organic matter in fluvial systems: a latitudinal study across Europe. Water Res. 144, 172–182.
Camargo, J.A., Alonso, A., 2006. Ecological and toxicological effects of inorganic nitrogen pollution in aquatic ecosystems: a global assessment. Environ. Int. 32 (6), 831–849.
Carrasco, L., Benejam, L., Benito, J., Bayona, J.M., Diez, S., 2011. Methylmercury levels and bioaccumulation in the aquatic food web of a highly mercury-contaminated reservoir. Environ. Int. 37 (7), 1213–1218.
Chen, W., Westerhoff, P., Leenheer, J.A., Booksh, K., 2003. Fluorescence excitation−emission matrix regional integration to quantify spectra for dissolved organic matter. Environ. Sci. Technol. 37 (24), 5701–5710.
Chiasson-Gould, S.A., Blais, J.M., Poulain, A.J., 2014. Dissolved organic matter kinetically controls mercury bioavailability to bacteria. Environ. Sci. Technol. 48 (6), 3153–3161.
Chow, C.W.K., Rolando, F., John, V.L., Dongsheng, W., Mary, D., 2008. Assessing natural organic matter treatability using high performance size exclusion chromatography. Environ. Sci. Technol. 42 (17), 6683–6689.
Christensen, G.A., Wymore, A.M., King, A.J., Podar, M., Hurt, R.A., Santillan, E.U., Soren, A., Brandt, C.C., Brown, S.D., Palumbo, A.V., Wall, J.D., Gilmour, C.C., Elias, D.A., 2016. Development and validation of broad-range qualitative and clade-specific quantitative molecular probes for assessing mercury methylation in the environment. Appl. Environ. Microbiol. 82 (19), 6068–6078.
Correia, R.R., Guimarães, J.R., 2016. Mercury methylation and sulfate reduction rates in mangrove sediments, Rio de Janeiro, Brazil: the role of different microorganism consortia. Chemosphere 167, 438–443.
Cuss, C.W., Guéguen, C., 2015. Relationships between molecular weight and fluorescence properties for size-fractionated dissolved organic matter from fresh and aged sources. Water Res. 68, 487–497.
Dignac, M.F., Ginestet, P., Rybacki, D., Bruchet, A., Urbain, V., Scribe, P., 2000. Fate of wastewater organic pollution during activated sludge treatment: nature of residual organic matter. Water Res. 34 (17), 4185–4194.
Driscoll, C.T., Chen, C.Y., Hammerschmidt, C.R., Mason, R.P., Gilmour, C.C., Sunderland, E.M., Greenfield, B.K., Buckman, K.L., Lamborg, C.H., 2012. Nutrient supply and mercury dynamics in marine ecosystems: a conceptual model. Environ. Res. 119 (5), 118–131.
French, T.D., Houben, A.J., Desforges, J.P.W., Kimpe, L.E., Kokelj, S.V., Poulain, A.J., Smol, J.P., Wang, X., Blais, J.M., 2014. Dissolved organic carbon thresholds affect mercury bioaccumulation in Arctic Lakes. Environ. Sci. Technol. 48 (6), 3162–3168.
Fu, X., Feng, X., Sommar, J., Wang, S., 2012. A review of studies on atmospheric mercury in China. Sci. Total Environ. 421-422 (1), 73–81.
Gascon, D.E., Loizeau, J.L., Cosio, C., Bouchet, S., Adatte, T., Amouroux, D., Bravo, A.G., 2016. Role of settling particles on mercury methylation in the oxic water column of freshwater systems. Environ. Sci. Technol. 50 (21), 11672–11679.
Ger, K.A., Urrutia-Cordero, P., Frost, P.C., Hansson, L.A., Sarnelle, O., Wilson, A.E., Lurling, M., 2016. The interaction between cyanobacteria and zooplankton in a more eutrophic world. Harmful Algae 54, 128–144.
Gilmour C.C., Podar M., Bullock A.L., Graham A.M., Brown S.D., Somenahally A.C., Johs A., Jr H.R., Bailey, K.L. and Elias, D.A., 2013. Mercury methylation by novel microorganisms from new environments. *Environ. Sci. Technol.* **47**(20), 11810–11820.
Han, C., Ding, S., Yao, L., Shen, Q., Zhu, C., Wang, Y., Xu, D., 2015. Dynamics of phosphorus-iron-sulfur at the sediment-water interface influenced by algae blooms decomposition. J. Hazard. Mater. 300, 329–337.
Hansson, L.A., 1988. Chlorophyll *a* determination of periphyton on sediments: identification of problems and recommendation of method. Freshw. Biol. 20 (3), 347–352.
He, T., Feng, X., Guo, Y., Qiu, G., Li, Z., Liang, L., Lu, J., 2008. The impact of eutrophication on the biogeochemical cycling of mercury species in a reservoir: a case study from Hongfeng Reservoir, Guizhou, China. Environ. Pollut. 154 (1), 56–67.
Herrero Ortega, S., Catalán, N., Björn, E., Gröntoft, H., Hilmarsson, T.G., Bertilsson, S., Wu, P., Bishop, K., Levanoni, O., Bravo, A.G., 2018. High methylmercury formation in ponds fueled by fresh humic and algal derived organic matter. Limnol. Oceanogr. 63, 544–553.
Hill, J.R., O'Driscoll, N.J., Lean, D.R.S., 2009. Size distribution of methylmercury associated with particulate and dissolved organic matter in freshwaters. Sci. Total

Environ. 408 (2), 408–414.
Hsu-Kim, H., Kucharzyk, K.H., Zhang, T., Deshusses, M.A., 2013. Mechanisms regulating mercury bioavailability for Methylating microorganisms in the aquatic environment: A critical review. Environ. Sci. Technol. 47 (6), 2441–2456.
Huang, J., Zhang, Y., Arhonditsis, G.B., Gao, J., Chen, Q., Wu, N., Dong, F., Shi, W., 2019. How successful are the restoration efforts of China's lakes and reservoirs? Environ. Int. 123, 96–103.
Huisman, J., Codd, G.A., Paerl, H.W., Ibelings, B.W., Verspagen, J., Visser, P.M., 2018. Cyanobacterial blooms. Nat. Rev. Microbiol. 16, 471–484.
Jeremiason, J.D., Reiser, T.K., Weitz, R.A., Berndt, M.E., Aiken, G.R., 2016. Aeshnid dragonfly larvae as bioindicators of methylmercury contamination in aquatic systems impacted by elevated sulfate loading. Ecotoxicology 25 (3), 456–468.
Jiang, X., Wang, S.H., Zhong, L.X., Jin, X.C., Sun, S.Q., 2010. Seasonal variation characteristics of algae biomass in Chaohu Lake. Environ. Sci. 31 (9), 2056–2062 (In Chinese).
Jiang, Y.J., He, W., Liu, W.X., Qin, N., Ouyang, H.L., Wang, Q.M., Kong, X.Z., He, Q.S., Yang, C., Yang, B., 2014. The seasonal and spatial variations of phytoplankton community and their correlation with environmental factors in a large eutrophic Chinese lake (Lake Chaohu). Ecol. Indic. 40 (5), 58–67.
Jun, Y.U., Zhang, X.S., Li, Y.C., Ning, W., 2016. Pollution characteristics and ecological risk of mercury in Hangbu-Fengle River of Chaohu Lake. China Environ. Sci. 36 (8), 2487–2494 (in Chinese).
Klapstein, S.J., O'Driscoll, N.J., 2018. Methylmercury biogeochemistry in freshwater ecosystems: a review focusing on DOM and photodemethylation. Bull. Environ. Contam. Toxicol. 100 (1), 14–25.
Kowalewska, G., 2005. Algal pigments in sediments as a measure of eutrophication in the Baltic environment. Quat. Int. 130 (1), 141–151.
Leclerc, M., Planas, D., Amyot, M., 2015. Relationship between extracellular low-molecular-weight thiols and mercury species in natural lake periphytic biofilms. Environ. Sci. Technol. 49 (13), 7709–7716.
Lee, J.H., Fredrickson, J.K., Kukkadapu, R.K., Boyanov, M.I., Kemner, K.M., Lin, X., Kennedy, D.W., Bjornstad, B.N., Konopka, A.E., Moore, D.A., 2012. Microbial reductive transformation of phyllosilicate Fe(III) and U(VI) in fluvial subsurface sediments. Environ. Sci. Technol. 46 (7), 3721–3730.
Lescord, G., Emilson, E., Johnston, T., Branfireun, B., Gunn, J., 2018. The optical properties of dissolved organic matter and their relation to mercury concentrations in water and biota across a remote freshwater drainage basin. Environ. Sci. Technol. 52 (6), 3344–3353.
Li, H., Hou, G., Feng, D., Xiao, B., Song, L., Liu, Y., 2007. Prediction and elucidation of the population dynamics of *Microcystis spp*. in Lake Dianchi (China) by means of artificial neural networks. Eco. Inform. 2 (2), 184–192.
Lin, Y., Larssen, T., Vogt, R.D., Feng, X., 2010. Identification of fractions of mercury in water, soil and sediment from a typical Hg mining area in Wanshan, Guizhou province, China. Appl. Geochem. 25 (1), 60–68.
Liu, B., Yan, H., Wang, C., Li, Q., Guédron, S., Spangenberg, J.E., Feng, X., Dominik, J., 2012. Insights into low fish mercury bioaccumulation in a mercury-contaminated reservoir, Guizhou, China. Environ. Pollut. 160 (1), 109–117.
Liu, Y.R., Johs, A., Bi, L., Lu, X., Hu, H.W., Sun, D., He, J.Z., Gu, B.H., 2018. Unraveling microbial communities associated with methylmercury production in paddy soils. Environ. Sci. Technol. 52 (22), 13110–13118.
Luengen, A.C., Fisher, N.S., Bergamaschi, B.A., 2012. Dissolved organic matter reduces algal accumulation of methylmercury. Environ. Toxicol. Chem. 31 (8), 1712–1719.
Luo, Y., Li, L., Li, Q., Jiao, S., Li, H., Chen, F., 2017. Spatial and temporal distribution of chlorophyll *a* and its relationship to algae and environmental factors in Aha Reservoir. Environ. Sci. 38 (10), 4151–4159 (in Chinese).
Ma, L., Zhong, H., Wu, Y.G., 2015. Effects of metal-soil contact time on the extraction of mercury from soils. Bull. Environ. Contam. Toxicol. 94 (3), 399–406.
Ma, M., Du, H., Wang, D., Sun, T., 2017. Mercury methylation in the soils and sediments of Three Gorges Reservoir Region. J. Soils Sediments 1–10.
Mangal, V., Stenzler, B.R., Poulain, A.J., Gueguen, C., 2019. Aerobic and anaerobic bacterial mercury uptake is driven by algal organic matter composition and molecular weight. Environ. Sci. Technol. 53 (1), 157–165.
Mazrui, N.M., Jonsson, S., Thota, S., Jing, Z., Mason, R.P., 2016. Enhanced availability of mercury bound to dissolved organic matter for methylation in marine sediments. Geochim. Cosmochim. Acta 194, 153–162.
Merel, S., Walker, D., Chicana, R., Snyder, S., Baures, E., Thomas, O., 2013. State of knowledge and concerns on cyanobacterial blooms and cyanotoxins. Environ. Int. 59, 303–327.
Noh, S., Kim, C.K., Kim, Y., Lee, J.H., Han, S., 2016. Assessing correlations between monomethylmercury accumulation in fish and trophic states of artificial temperate reservoirs. Sci. Total Environ. 580, 912–919.
Olsen, T.A., Brandt, C.C., Brooks, S.C., 2016. Periphyton biofilms influence net methylmercury production in an industrially contaminated system. Environ. Sci. Technol. 50 (20), 10843–10850.
Parks, J.M., Johs, A., Podar, M., Bridou, R., Jr, H.R., Smith, S.D., Tomanicek, S.J., Qian, Y., Brown, S.D. Brandt, C.C. 2013. The genetic basis for bacterial mercury methylation. Science, 339(6125), 1332–1335.
Pickhardt, P.C., Folt, C.L., Chen, C.Y., Klaue, B., Blum, J.D., 2002. Algal blooms reduce the uptake of toxic methylmercury in freshwater food webs. Proc. Natl. Acad. Sci. U. S. A. 99 (7), 4419–4423.
Santisteban, J.I., Mediavilla, R., López-Pamo, E., Dabrio, C.J., Zapata, M.B.R., García, M.J.G., Castaño, S., Martínez-Alfaro, P.E., 2004. Loss on ignition: a qualitative or quantitative method for organic matter and carbonate mineral content in sediments? J. Paleolimnol. 32 (3), 287–299.
Soerensen, A.L., Schartup, A.T., Gustafsson, E., Gustafsson, B.G., Undeman, E., Björn, E., 2016. Eutrophication increases phytoplankton methylmercury concentrations in a coastal sea-a Baltic Sea case study. Environ. Sci. Technol. 50 (21), 11787–11796.
Tang, Y., Zhang, M., Sun, G., Pan, G., 2019. Impact of eutrophication on arsenic cycling in freshwaters. Water Res. 150, 191–199.
Tao, Y., Xue, B., Zhong, J., Yao, S., Wu, Q., 2012. Influences of pH, heavy metals and phosphate and their co-influences on the sorption of pentachlorophenol on cyanobacterial biomass. Water Res. 46 (11), 3585–3594.
Tavshunsky, I., Eggert, S.L., Mitchell, C.P.J., 2017. Accumulation of methylmercury in invertebrates and masked shrews (Sorex cinereus) at an upland forest-peatland interface in Northern Minnesota, USA. Bull. Environ. Contam. Toxicol. 99 (6), 673–678.
Tong, H., Hu, M., Li, F.B., Liu, C.S., Chen, M.J., 2014. Biochar enhances the microbial and chemical transformation of pentachlorophenol in paddy soil. Soil Biol. Biochem. 70 (2), 142–150.
Tsui, M.T.K., Finlay, J.C., Balogh, S.J., Nollet, Y.H., 2010. In situ production of methylmercury within a stream channel in Northern California. Environ. Sci. Technol. 44 (18), 6998–7004.
USEPA, 1998. Method 7473: Mercury in Solids and Solutions by Thermal Decomposition, Amalgamation and Atomic Spectrophotometry. Washington, DC.
USEPA, 2001. Method 1630: Methylmercury in water by distillation, aqueous ethylation, purge and trap, and CVAFS. In: EPA-821-R-01-020 USEPA. DC, Washington.
Wang, S.R., 2015. Chinese Lakes Environment Evolution and Management Strategy. Science Press, Beijing.
Wang, Y.J., Dang, F., Zhao, J.T., Zhong, H., 2016. Selenium inhibits sulfate-mediated methylmercury production in rice paddy soil. Environ. Pollut. 213, 232–239.
Xing, L., Murshed, M.F., Lo, T., Fabris, R., Chow, C.W.K., Leeuwen, J.V., Drikas, M., Wang, D., 2012. Characterization of organic matter in alum treated drinking water using high performance liquid chromatography and resin fractionation. Chem. Eng. J. 192 (2), 186–191.
Yan, H., Li, Q., Meng, B., Wang, C., Feng, X., He, T., Dominik, J., 2013. Spatial distribution and methylation of mercury in a eutrophic reservoir heavily contaminated by mercury in Southwest China. Appl. Geochem. 33 (1), 182–190.
Yu, G., Jiang, Y., Song, G., Tan, W., Zhu, M., Li, R., 2014. Variation of microcystis and microcystins coupling nitrogen and phosphorus nutrients in Lake Erhai, a drinking-water source in Southwest Plateau, China. Environ. Sci. Pollut. Res. 21 (16), 9887–9898.
Zeng, L., Luo, G., He, T., Guo, Y., Qian, X., 2016. Effects of sulfate-reducing bacteria on methylmercury at the sediment-water interface. J. Environ. Sci. 46 (8), 214–219.
Zhang, W., Yang, P., Yang, X., Chen, Z., Wang, D., 2015. Insights into the respective role of acidification and oxidation for enhancing anaerobic digested sludge dewatering performance with Fenton process. Bioresour. Technol. 181, 247–253.
Zhang, Y., Liu, Y.R., Lei, P., Wang, Y.J., Zhong, H., 2018. Biochar and nitrate reduce risk of methylmercury in soils under straw amendment. Sci. Total Environ. 619-620, 384–390.
Zhao, J.Y., Ye, Z.H. Zhong, H. 2018. Rice root exudates affect microbial methylmercury production in paddy soils. Environmental pollution, 242(Pt B), 1921-1929.
Zhao, Y.P., Zhang, Z.Q., Wang, G.X., Li, X.J., Ma, J., Chen, S., Deng, H., Annalisa, O.H., 2019. High sulfide production induced by algae decomposition and its potential stimulation to phosphorus mobility in sediment. Sci. Total Environ. 650, 163–172.
Zhong, H., Wang, W.X., 2010. Methylmercury extraction from artificial sediments by the gut juice of the sipunculan, Sipunculus nudus. Environ. Toxicol. Chem. 27 (1), 138–145.
Zhu, H., Zhong, H., Wu, J., 2016. Incorporating rice residues into paddy soils affects methylmercury accumulation in rice. Chemosphere 152, 259–264.